

Creep failure strain estimation of glass fibre/polypropylene composites based on short-term tests and Weibull characterisation

Vas L. M., Bakonyi P.

Accepted for publication in Journal of Reinforced Plastics and Composites

Published in 2013

DOI: [10.1177/0731684412453513](https://doi.org/10.1177/0731684412453513)

Creep Failure Strain Estimation of GF/PP Composites Based on Short Term Tests and Weibull Characterization

László Mihály Vas*, Péter Bakonyi

Department of Polymer Engineering, Faculty of Mechanical Engineering, Budapest University of Technology and Economics, HU-1111 Budapest, Műegyetem rkp 3, Hungary

Corresponding author's: E-mail: vas@pt.bme.hu Tel: (+36)14631529

Abstract

In order to study the short and long term creep behaviours of injection moulded unreinforced and glass fibre reinforced PP composites, tensile and creep measurements were carried out and analysed. Based on the linear viscoelastic behaviour and variable transformations as well as Weibull-based distribution characterization estimations for the tensile strength parameters and creep failure strain were determined and fitted to the measurements. These mathematical estimations and the relationships between the material model constants and the fibre content, determined by fitting, give a possibility for designers' calculations at arbitrary creep load levels and fibre contents.

Keywords:

short term creep, long term behaviour, creep failure strain, PP composite, Weibull distribution

1 INTRODUCTION

The short and long term creep behaviour is one of the most important properties of polymers used for engineering applications. Therefore, it has been studied for a long time in order to find suitable estimation methods.

On the basis of linear viscoelastic and simple thermo-rheological behaviour, the time-temperature superposition principle can be used to construct the long term creep curve, called master-curve, from short term creep measurements performed at different temperatures and at a given load level.¹⁻¹⁰ To

extrapolate the measured data or to describe the master curve mathematically, power law type approximations such as: Nutting or Findley^{6,8,11} or simple rheological models^{1-5,12}, can give a simple solution. In some cases, constitutive mathematical or finite element mechanical models^{13,14} or molecular chain based structural models¹⁵ are developed to predict creep in polymers. In general, these methods can be used just at (or below) a given load level and in most cases, they cannot estimate the expected lifetime and/or the creep failure strain.

A combined method based on the linear viscoelastic theory and non-linear variable transformations has been developed for estimating the long term behaviour from short term measurements, by Nagy and Vas^{16,17}. This method was applied to estimate the tensile strength parameters and the creep failure strain of unreinforced PP at arbitrary load levels, by making use of the information provided from tensile tests and short term creep measurements as well as a Weibull-based distribution stochastic model.¹⁸ In this paper, this examination is extended for glass fibre reinforced PP composites.

2 THEORETICAL CONSIDERATIONS

The method used for estimating the creep failure strain values at arbitrary load levels, was developed and applied¹⁸ to PP earlier.

It is based, essentially, on short term measurements, such as constant load rate tensile tests and creep tests for a maximum of 10 hours, performed at different load levels and a model including linear viscoelastic estimations and their non-linear variable transformation, similar to that used in the case of the time-temperature superposition principle. The calculations, supported by a Weibull-based distribution stochastic model, are carried out using the following formulae.

The measured tensile test curve, $\varepsilon_2(t)$, can be described by a Weibull-based distribution approximation:

$$\varepsilon_2(t) \approx \varepsilon_{L2}(t) = \varepsilon_{2B} - \varepsilon_{L1B\infty} \left(1 - e^{-\left(\frac{t_{2B}-t}{a}\right)^k} \right), 0 \leq t \leq t_{2B} \quad (1)$$

where t_{2B} is the breaking time in tensile testing, hence $\varepsilon_{2B}=\varepsilon_2(t_{2B})$ is the strain-at-break, while ‘a’ and ‘k’ are the Weibull scale and modulus factors, respectively and $\varepsilon_{L1B\infty}$ is an asymptotic strain value used in the case of creep.

In the case of real creep stimulus (Figure 1(a)), the primary linear viscoelastic (LVE) response, $\varepsilon_{L1}(t)$, estimation of the real creep curve and its Weibull-based distribution approximation¹⁶⁻¹⁸ (Figure 1(b)) are as follows:

$$\varepsilon_{L1}(t, t_0) = \varepsilon_2(t) - \varepsilon_2(t - t_0) \approx \varepsilon_{L1B\infty} \left(e^{-\left(\frac{t_{2B}-t}{a}\right)^k} - e^{-\left(\frac{t_{2B}-t+t_0}{a}\right)^k} \right), t_0 \leq t \leq t_{2B} \quad (2)$$

where t_0 is the uploading time in a creep tests, and $\varepsilon_{L1}(t, t_0) = \varepsilon_2(t_0) = \varepsilon_0$ is the creep strain load.

Setting the time at t_{2B} in equation (2), gives $\varepsilon_{L1}(t_{2B}) = \varepsilon_{L1B}(t_0)$ that yields the relationship between the LVE creep failure strain and uploading time:

$$\varepsilon_{L1B}(t_0) = \varepsilon_{L1}(t_{2B}, t_0) \approx \varepsilon_{L1B\infty} \left(1 - e^{-\left(\frac{t_0}{a}\right)^k} \right), 0 \leq t_0 \leq t_{2B} \quad (3)$$

Subtracting the strain loads, ε_0 , from values $\varepsilon_{L1B}(t_0)$ results in a nearly symmetric curve that has got a maximum.

$$\varepsilon_{L1B}(t_0) - \varepsilon_0 = \varepsilon_{L1B\infty} \left(1 - e^{-\left(\frac{t_0}{a}\right)^k} + e^{-\left(\frac{t_0}{a}\right)^k} - e^{-\left(\frac{t_{2B}-t_0}{a}\right)^k} \right), 0 \leq t_0 \leq t_{2B} \quad (4)$$

The real creep curve, $\varepsilon_1(t)$, can be estimated by a non-linear variable transformation (T) of the primary LVE estimation, $\varepsilon_{L1}(t)$:

$$\varepsilon_1(t) \approx T_1(\varepsilon_{L1}(T_2(t))) = \varepsilon_{L11}(T_2(t)) \quad (5)$$

where T_1 and T_2 are the component transformations (Figure 1(b)) and $\varepsilon_{L11}(t)$ is defined by equation (5). T_2 is determined to be non-linear, however, T_1 can be realised in a linear form; consequently $\varepsilon_{L11}(t)$ is the secondary LVE estimation of $\varepsilon_1(t)$ that is given by equation (6):

$$\varepsilon_{L11}(t) = T_1(\varepsilon_{L1}(t)) = \varepsilon_{L1}(t_0) + c(\varepsilon_{L1}(t) - \varepsilon_{L1}(t_0)) = \varepsilon_0 + c(\varepsilon_{L1}(t) - \varepsilon_0) \quad (6)$$

where 'c' is a constant and ε_0 is defined by equation (7):

$$\varepsilon_0 = \varepsilon_{L1}(t_0) = \varepsilon_2(t_0) \quad (7)$$

If t_{1B} is the real lifetime in a creep experiment, hence the creep failure strain is $\varepsilon_{1B} = \varepsilon_1(t_{1B})$, which can be estimated by equation (8):

$$\varepsilon_{1B} \approx \varepsilon_{L11}(t_{2B}, t_0) = T_1(\varepsilon_{L1}(t_{2B}, t_0)) = \varepsilon_0 + c(\varepsilon_{L1}(t_{2B}, t_0) - \varepsilon_0) \quad (8)$$

In this paper, it will be shown that this method can also be applied to glass fibre reinforced PP polymers and the formulae can be extended for different fibre contents over a wide range.

3 MATERIALS AND TEST METHODS

An isotactic polypropylene homopolymer (melting point: 165°C; density: 0.9 g/cm³) (Tipplen H949A, TVK, Hungary) and its glass fibre reinforced composites were subjected to tensile tests, at constant force rate and creep measurements. Matrix material, 4.5 mm long chopped E-glass fibres (diameter: 13 µm) (SV EC 13 473, Johns Manville, Czech Republic) and maleic anhydride grafted PP (melting point: 167°C; density: 0.905 g/cm³) (Orevac CA100, Arkema, France) of 2% GF contents were mixed in a twin-screw extruder (Brabender Plasti-Corder, USA). Pellets with 0, 5, 10, 20, 30 and 40% glass fibre content were produced with zone temperatures of 190-210-210-230°C (from hopper to die). To achieve a similar thermal prehistory as that of the glass fibre reinforced PP composites, the unreinforced material was regranulated with the same settings.¹⁸ 148 mm long, type 1A, dumbbell specimens of 10 mm width and 4 mm thickness, according to the ISO 527-2 standard, were injection moulded on an Arburg Allrounder

320C 500-170 (Germany) injection moulding machine with zone temperatures of 170-175-180-185-190°C, 50 cm³/s injection rate and from the fibre content dependent injection (700-1000 bar) and holding (500-700 bar) pressures.

For the tests, a Zwick Z-005 universal tensile testing machine (with 5 kN nominal capacity standard load cell) was used in constant force rate mode, where force rate was 50 N/s, until the specimen broke in tensile tests or the preset load level was reached in creep tests. The gauge length was 100 mm long, hence the elongation in millimetre equals, numerically, to the strain in percent. In the creep tests, after the uploading, the load was held constant for 10 hours (or until the specimen failed) and the length variation of the specimen was measured, using the crosshead signal. The applied load levels were determined in 10 or 5 percent steps of the averaged breaking force measured for the given materials (neat PP, 30%GF/PP composite).

4 MEASUREMENTS

Thirty constant force rate tensile tests were performed on injection moulded dumbbell specimens. At the starting phase of uploading, due to the inertia of the engine system of the universal testing machine and the time-delay of the data collection, a zero-point error can be observed which could cause serious anomalies in calculating the correct mean curves. In order to obtain the correct averaged characteristics, the curves were shifted one by one as a function of time, until the initial tangents of the measured strain-time and force-time curves crossed exactly the origin and some starting points were corrected to fit into the initial tangent as it was done in a previous work dealing with neat PP.¹⁸ The corrected results of the tensile measurements were averaged point by point and smoothed in the breaking section.¹⁸ The averaged curves, together with the breaking points, are depicted in Figure 2.

The average values of the breaking strain and force values with their standard deviations are summarized in Table 1.

In the case of the neat PP and 30% GF reinforced composites, five creep measurements were performed at every load level that were 10, 20, 30, 40, 50, 60, 65, 70, 75, 80, 85, 90 and 95% of the mean

breaking force (Table 1). Each creep test lasted 10 hours or until the specimen failed. The curves were averaged point by point in the manner described above and smoothened, if necessary (where the specimen was broken during the creep measurement).

The averaged and smoothed creep curves of the 0%GF and 30%GF reinforced PP materials can be seen in Figures 3 and 4, where all the creep failure points observed are also depicted.

5 EVALUATION AND DISCUSSION

The first step of the Weibull-based method was developed and applied in an earlier paper.¹⁸ This step was employed in determining the first LVE estimation of the creep failure strain values, $\varepsilon_{L1}(t_{2B})$, from the measured and averaged strain-time curve, $\varepsilon_2(t)$, recorded by tensile test using equations (2) and (3). This was followed by fitting the right hand side of equation (3), to the curve $\varepsilon_{L1B}(t_0)=\varepsilon_{L1}(t_{2B}, t_0)$.

5.1 Estimation of LVE creep failure strain based on Weibull distribution

In all cases, the fitting was carried out by calculating the linear regression in a double logarithmic coordinate system. Figure 5 shows the LVE estimation of the creep failure strain as a function of the uploading time (t_0), determined from the measured tensile test curve and its Weibull-based approximation fitted by using equation (3).

The excellent agreement with the measurements is confirmed by the high coefficients of fit ($R^2>0.995$), where the fitting parameters are: a , k , and $\varepsilon_{L1B\infty}$.

5.2 Weibull-based distribution approximation of the tensile test curve

Knowing the fitted parameters (Table 2), the Weibull-based distribution approximation of the measured strain-time curves could be calculated according to equation (1). The measured and modelled tensile test curves are in good agreement, as can be seen in Figure 6.

5.3 Relation between creep failure strain increment and load level

The net creep strain that is the strain increment arising after uploading, when the load is constant, is the difference of the resultant strain $\varepsilon_1(t)$ measured and the strain load level, ε_0 . In accordance with that, in Figure 7, the LVE creep failure strain increment calculated according to equation (4) is plotted for the materials tested as a function of the uploading time (Figure 7(a)) or the creep strain level (Figure 7(b)). The curves that were computed from the measurements and the Weibull-based distribution approximations exhibit a maximum creep strain value at about half the tensile test time ($t_0 \approx t_{2B}/2$) (Figure 7(a)) or about 1.0-1.5% creep load level.

5.4 Estimation of the measured creep failure strain

The LVE estimation of the real creep failure strain, $\varepsilon_{1B}(t_0)$, belonging to uploading time, t_0 , is $\varepsilon_{L1B}(t_0) = \varepsilon_{L1}(t_{2B})$, where t_{2B} is the mean value of the fracture times obtained by tensile measurements. On the basis of the creep measurements done at higher strain load levels, these $\varepsilon_{L1B}(t_0)$ values can be considered as upper estimations of the measured values for the unreinforced PP (Figure 8(a)), while in the case of the widely used 30%GF reinforced PP (Figure 8(b)), a curve defined by these modelled values, passes the measured values.

Applying variable transformation T_1 along the strain axis according to equations (5) to (8), provides the first non-linear viscoelastic approximation (NLVE) of the real creep curve ($\varepsilon_{L11}(t)$). Numerical examinations¹⁶⁻¹⁸ showed that in this case, transformation T_1 could be realised as a linear combination using a permanent transformation parameter, $0 < c$. Consequently, the result can be considered to be the secondary LVE estimation of the creep curve. The value of this new approximation of the creep curve set at t_{2B} , estimates the real creep failure strain, $\varepsilon_{1B} = \varepsilon_1(t_{1B})$, observed at instant t_{1B} of the creep failure, as an average.

Fitting the measured values of the creep failure strain by using the least square method, the transformation parameter, c , came to about 0.70 for the neat PP (Figure 8(a))¹⁸ and to about 1.06 in case of the 30% GF reinforced PP (Figure 8(b)). In contrast to the neat PP, the secondary estimation of the creep failure strain for the composites is close to the primary estimations.

5.5 Relationships between the parameters and the fibre content

Knowing the measured values that characterize the strength and the fitted parameters of the Weibull-based distribution approximations, it is essential and beneficial to seek suitable analytical relationships between them and the fibre content.

Figure 9 shows the measured values of the mean breaking strain ($y=\varepsilon_{2B0}$) and calculated values of the maximum of the creep failure strain increment ($y=\varepsilon_{1BM}$) and the asymptotic values of the mean creep failure strain ($y=\varepsilon_{1B\infty}$) as a function of the fibre content ($0\leq\varphi\leq 40\%$) as well as their approximation computed from equation (9) as the linear contribution of two exponential functions:

$$y(\varphi) = y_0 + y_1 e^{-\frac{\varphi}{b_1}} + y_2 e^{-\frac{\varphi}{b_2}} \quad (9)$$

The constants (y_{012} , y_1 , y_2 , b_1 , b_2 ,) obtained from the fitting are summarized in Table 3. The coefficient of fit is characterized by high values (Table 3).

The breaking time (t_{2B}) versus fibre content relation could be described by linear regression (equation (10)) with good agreement ($R^2=0.987$) in the range $0\leq\varphi\leq 40\%$ (Figure 10). It is also true to the time (t_{1M}) belonging to the maximum value of the creep failure strain increment ($R^2=0.986$) (Figure 10).

$$\begin{aligned} t_{2B} &\approx T_{20} + T_{21}\varphi \\ t_{1M} &\approx T_{10} + T_{11}\varphi \end{aligned} \quad (10)$$

In equation (10), fitted constants translated to: $T_{20}=33.42$ s, $T_{21}=1.247$ s/%, $T_{10}=16.71$ s, $T_{11}=0.6234$ s/%.

Since the tensile force is proportional to the time, because of the constant rate load mode. These linear approximations can also be applied to the force versus fibre content relations.

The variation of the Weibull parameters as a function of the fibre content is visible in Figure 11. The scale factor increases monotonically and a similar behaviour can be assumed for the modulus factor. In the case of the scale factor, a double exponential function gives appropriate approximation ($0\leq\varphi\leq 40\%$) (equation (11)):

$$a(\varphi) = a_{\infty} e^{-be^{-c\varphi}} \quad (11)$$

where the fitted constants are $a_{\infty}=189$ s, $b=3.15$, $c=0.125$ and the coefficient of fit is given by $R^2=0.9948$.

The changes of the modulus-factor could be estimated by an exponential function ($0 \leq \varphi \leq 40\%$) (equation (12)):

$$k(\varphi) = k_0 + (k_{\infty} - k_0)(1 - e^{-c\varphi}) = k_{\infty} + (k - k_0)e^{-c\varphi} \quad (12)$$

with the constants $k_0=0.5875$, $k_{\infty}=0.718$, $c=0.2$ and the determination coefficient was $R^2=0.714$ ($R=0.845$).

5.6 Assessment of the extreme behaviour of composites

The Weibull-based characterization of the glass fibre reinforced PP composites in the tested range of fibre content and the analysis of the fibre content dependency of the parameters, make it possible to estimate any of the mechanical characteristics obtainable by tensile or creep tests at arbitrary creep load levels or fibre contents. On the other hand, it also gives a possibility to assess the behaviour of the composites outside the fibre content range tested, by using extrapolation based on the fitted parameter versus fibre content relationships because all of them can be defined in the whole range of the fibre content. This means that examining the behaviour of composites at large fibre contents, even at 100% is possible. The latter leads to a material that consists of short fibres only, but the adhesion operates among the fibres. For this extreme case, the mean breaking strain, the asymptotic values of the mean creep failure strain and the maximum of the creep failure strain increment may be $\varepsilon_{2B}(100) \approx 2.81\%$, $\varepsilon_{1B\infty}(100) \approx 7.21\%$, and $\varepsilon_{1BM}(100) \approx 1.01\%$, while the mean breaking time and the creep time belonging to the maximum creep strain increment are: $t_{2B}(100) \approx 158$ s and $t_{1M}(100) \approx 79$ s, respectively.

According to Bobeth¹⁹, the mean breaking strain and strength of glass fibres are about 1-4% and 2.5-3.5 GPa, respectively. The mean breaking strain value corresponds to this value, but the mean breaking strength that can be calculated from the mean breaking time (t_{2B}), the load rate ($\dot{F}_0 = 50$ N/s) and the initial

cross section area ($A_0=40 \text{ mm}^2$), $\sigma_{2B}(100)\approx \dot{F}_o t_{2B}(100)/A_0=198 \text{ MPa}$, is less by an order of magnitude. It seems realistic because the latter is not that of the glass fibre, but just of a short fibre system characterized by the adhesion between fibres and matrix and the mean fibre length.

For the Weibull parameters, in this extreme case, the respective assessments for the scale and modulus factors are: $a(100)\approx 189 \text{ s}$ and $k(100)\approx 0.718$. They are essentially the asymptotic values of the parameters.

6 CONCLUSION

Injection moulded PP and glass fibre reinforced PP composite specimens were tested using tensile and short term creep tests in order to analyse the creep behaviour as a function of the fibre content. Using an LVE formula developed earlier, the creep failure strain values were estimated from the mean tensile test curve obtained by averaging the zero-point-corrected strain-time curves for each material tested. Weibull-based distribution stochastic model was used to describe the variation of the mean values of these failure strain estimations as a function of the uploading time or the creep load level, where the parameters were found by fitting the measurements. This made it possible to determine the approximation for the mean tensile test curve as well. The linear variable transformation of the LVE strain characteristics allows estimations to be determined for the measured creep failure strain values in the cases of the unreinforced PP and 30%GF/PP composite.

The relationships between the material model constants and the fibre content determined by fitting, give a possibility for designers' calculations at arbitrary creep load levels and fibre contents. Assessments of the extreme behaviour at 100% fibre content could be adjudged to be real.

The Weibull-based mathematical approximation distribution applied for unreinforced and reinforced PP materials, gives a good basis for developing the non-linear time-transformation necessary for the short term tests based on the estimation of the long term creep behaviour and the expected lifetime.

Acknowledgements

This work is connected to the scientific program of the "Development of quality-oriented and harmonized R+D+I strategy and functional model at BME" and "Talent care and cultivation in the scientific workshops of BME" projects. This project was supported by the New Széchenyi Plan [grant numbers: TÁMOP-4.2.1/B-09/1/KMR-2010-0002, TÁMOP-4.2.2.B-10/1-2010-0009] and the OTKA Hungarian Scientific Research Fund [grant numbers: K68438, K100469].

References

1. Ward IM, Hadley DW. Mechanical Properties of Solid Polymers, Chichester: Wiley, 1995.
2. Ehrenstein GW. Polymerwerkstoffe – Struktur und mechanisches Verhalten. München: Hanser, 1978.
3. Nielsen LE, Landel RF. Mechanical Properties of Polimers and Composites. New York: Marcel Dekker, 1994.
4. Retting W. Mechanik der Kunststoffe, München: Hanser, 1992.
5. Urzumtsev JS, Maksimov RD. Deformation of Plastics (in Hungarian), Budapest: Műszaki Könyvkiadó, 1982.
6. Dutta PK, Hui D. Creep rupture of a GFRP composite at elevated temperatures. *Comput. Struct.* 2000; 76: 153–161.
7. Guo YC, Xin CL, Song MS, He YD. Study on Short- and Long-Term Creep Behavior of Plastics Geogrid, *Polym. Test.* 2005; 24: 793–798.
8. Siengchin S, Karger-Kocsis J. Structure and creep response of toughened and nanoreinforced polyamides produced via the latex route: Effect of nanofiller type, *Compos. Sci. Technol.* 2009; 69: 677–683.
9. Izer A, Bárány T. Effect of consolidation on the flexural creep behaviour of all-polypropylene composite, *Exp. Poly. Lett.* 2010; 4: 210–216.
10. Pandini S, Pegoretti A. Time and temperature effects on Poisson's ratio of poly(butylene terephthalate). *Exp. Poly. Lett.* 2011; 5: 685–697.
11. Rees DWA. Nutting Creep in Polymer Composites, *J. Mater. Process. Technol.* 2003; 143: 164–170.
12. Banik K. Effect of mold temperature on short and long-term mechanical properties of PBT. *Exp. Poly. Lett.* 2008; 2: 111–117.
13. Drozdov AD. Creep Rupture and Viscoelasticity of Polypropylene. *Eng. Fract. Mech.* 2010; 77: 2277–2293.
14. Chung PW, Tamma KK, Namburu RR. A finite element thermo-viscoelastic creep approach for heterogeneous structures with dissipative correctors. *Finite Elem. Anal. Des.* 2000; 36: 279–313.
15. Baltussen JJM, Northolt MG. The viscoelastic extension of polymer fibres – creep behavior. *Polymer* 2001; 42: 3835–3846.
16. Nagy P, Vas LM. Investigating the Time Dependent Behavior of Thermoplastic Polymers under Tensile Load. In: *Macromolecular Symposia Special Issue: Adv. Polym. Compos. Technol.* 2006; 239: 176–181.
17. Nagy P, Vas LM. Relationship between Constant Strain Rate and Stress Relaxation Behavior of Polypropylene. *Exp. Poly. Lett* 2007; 1: 84–91.

18. Vas LM, Bakonyi P. Estimating the Creep Failure Strain of PP at Different Load Levels Based on Short Term Tests and Weibull Characterization. (Submitted to Exp. Poly. Lett on 13.04.2012.) 1-12.
19. Bobeth W. Textile Faserstoffe. Beschaffenheit und Eigenschaften. Berlin: Springer, 1993.

Table 1. Mean breaking strain and force values of the materials tested

Material	Breaking strain [%]	Breaking force [N]
Neat PP	11.17 ± 0.73	1619 ± 20
5% GF reinforced PP	4.87 ± 0.13	1884 ± 11
10% GF reinforced PP	3.94 ± 0.22	2350 ± 22
20% GF reinforced PP	3.49 ± 0.17	3095 ± 49
30% GF reinforced PP	3.22 ± 0.09	3572 ± 58
40% GF reinforced PP	3.03 ± 0.10	4050 ± 55

Table 2. The parameters of the breaking point and the Weibull-based distribution approximation

Fibre content, GF%	0	5	10	20	30	40
Breaking time, t_{2B} [s]	32,4	37,7	47,0	61,9	71,4	81,0
Breaking strain, ε_{2B} [%]	11,17	4,87	3,94	3,49	3,22	3,03
Asymp. failure strain, $\varepsilon_{1B\infty}$ [%]	12,47	8,13	7,61	8,29	7,85	6,99
Weibull modulus-factor, k [-]	0,5875	0,6675	0,7416	0,7434	0,6938	0,6765
Weibull scale-factor, a [s]	8,08	43,21	71,98	139,60	179,83	186,22
Creep strain maximum, ε_{1M} [%]	8,23	2,24	1,44	1,13	1,15	1,16
Time, $t_{1M}(\varepsilon_{1M})$ [s]	16,2	18,8	23,5	31,0	35,7	40,5
t_{B2}/a [-]	1,383	0,113	0,055	0,025	0,018	0,016

Table 3. Fitted parameters of the approximations in Figure 9

Property, y	y_0 [%]	y_1 [%]	y_2 [%]	b_1 [%]	b_2 [%]	R^2 [-]
ε_{2B}	2.8	6.367	2	2	18.65	0.9998
ε_{1BM}	1	6	1	1.5	20	0.9859
$\varepsilon_{1B\infty}$	7.2	3.9	1.4	1.5	20	0.9545

Figure 1. Stimuli of real creep and tensile tests (a) and the responses with the LVE estimation of the real creep curve (b)¹⁸

Figure 2. Tensile test curve of the neat PP and its composites

Figure 3. Creep results carried out on neat PP at different tensile load levels¹⁸

Figure 4. Creep results carried out on 30%GF/PP composite at different tensile load levels

Figure 5. LVE estimation of the creep failure strain calculated from the tensile test measurements and Weibull-based distribution model fitted

Figure 6. Averaged tensile test curves and their Weibull distribution based approximation

Figure 7. Weibull-based distribution LVE estimation and the measured values of the creep failure strain versus the uploading time (a) and the strain load level (b)

Figure 8. Measured values of the creep failure strain versus the uploading time and their primary and the secondary LVE estimations for the neat PP (a) and the 30%GF/PP composite (b)

Figure 9. Measured and modelled breaking strain, asymptotic value of the creep failure strain and maximum value of the creep strain increment versus fibre content

Figure 10. Measured and approximated values of the breaking time and the creep time belonging to the maximum of the creep strain increment versus fibre content

Figure 11. Scale (a) and modulus (b) factors versus fibre content

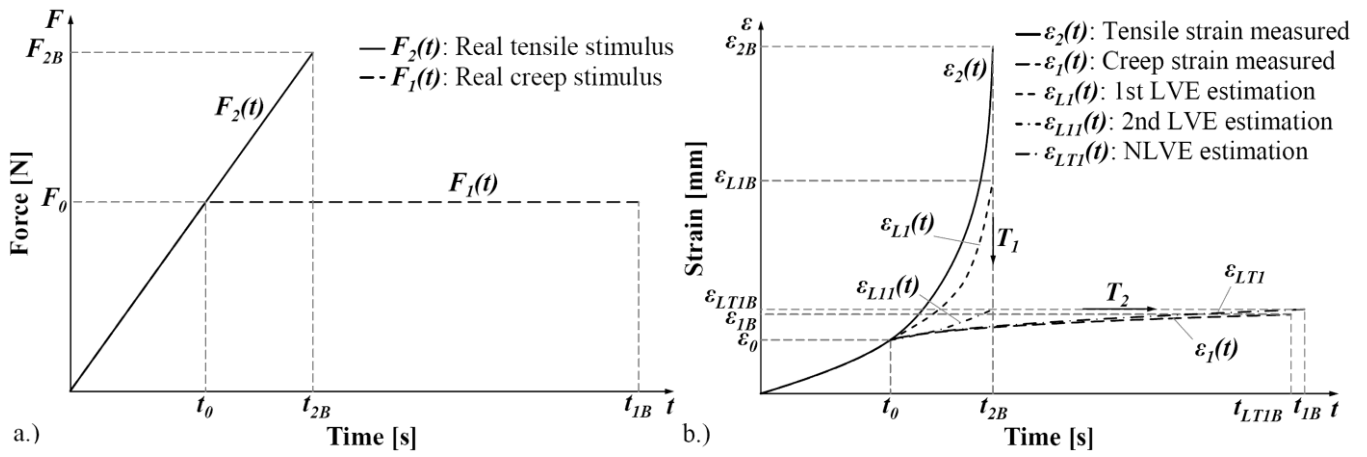


Figure 1. Stimuli of real creep and tensile tests (a) and the responses with the LVE estimation of the real creep curve (b)¹⁸

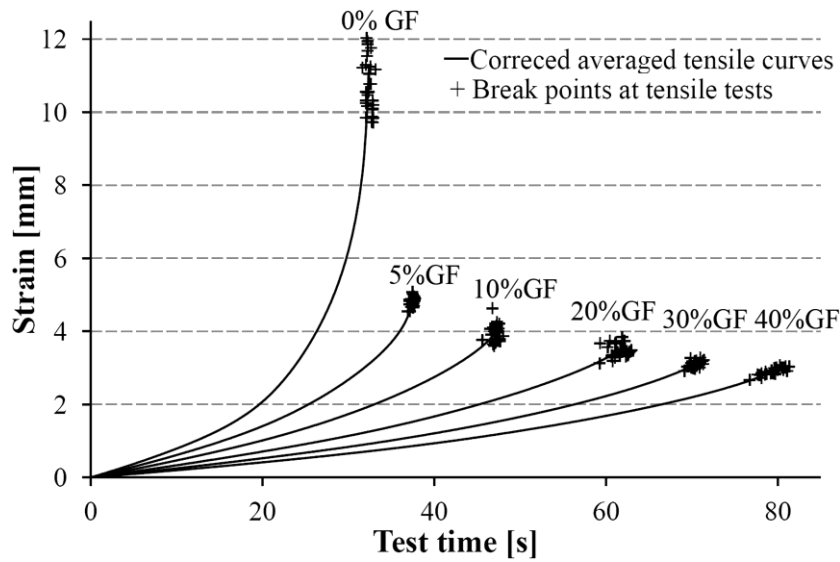


Figure 2. Tensile test curve of the neat PP and its composites

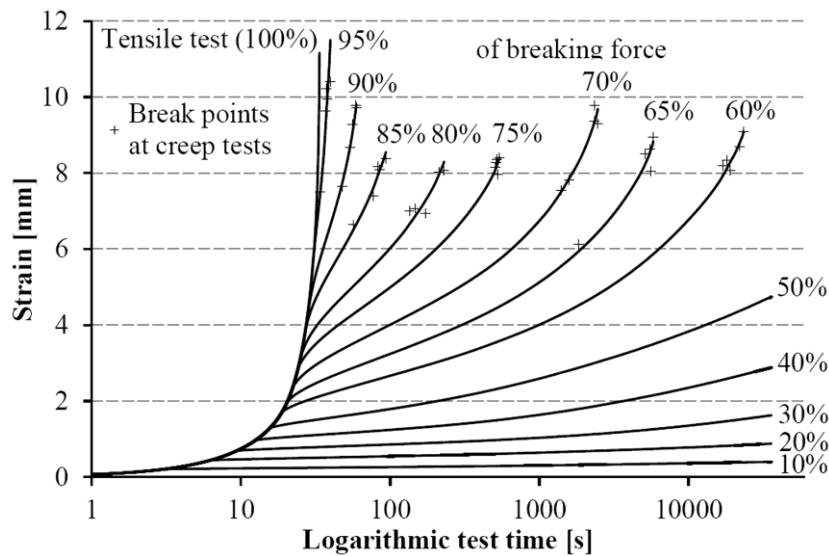


Figure 3. Creep results carried out on neat PP at different tensile load levels¹⁸

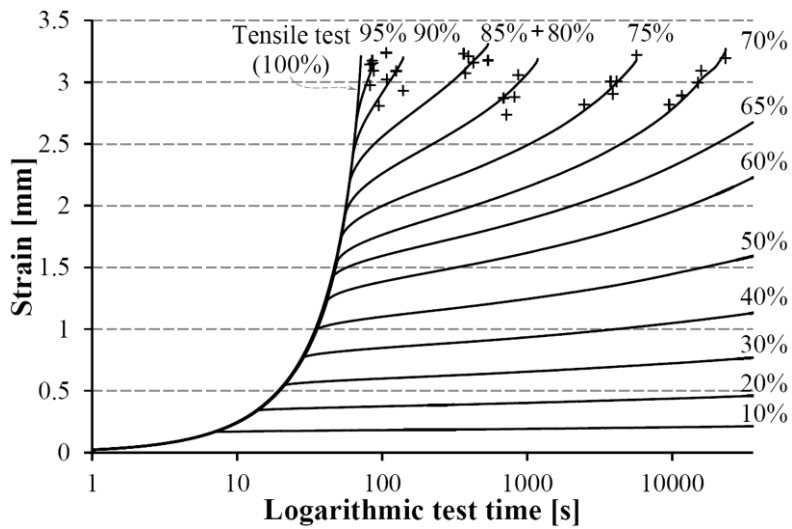


Figure 4. Creep results carried out on 30%GF/PP composite at different tensile load levels

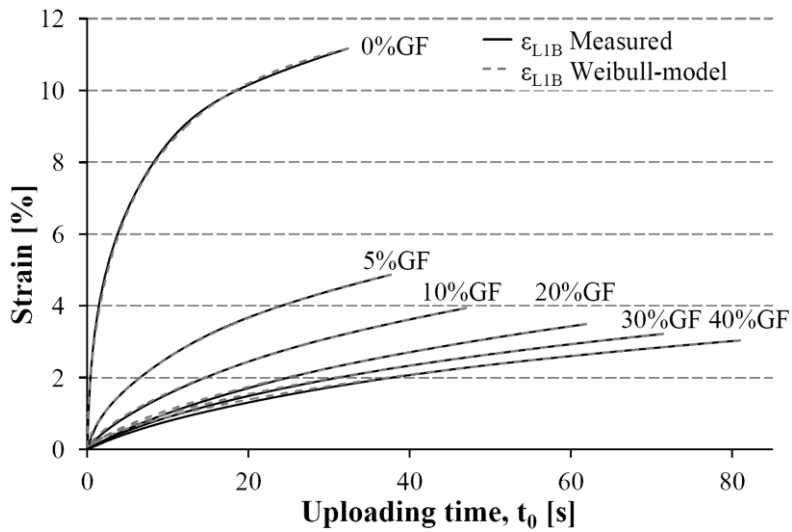


Figure 5. LVE estimation of the creep failure strain calculated from the tensile test measurements and Weibull-based distribution model fitted

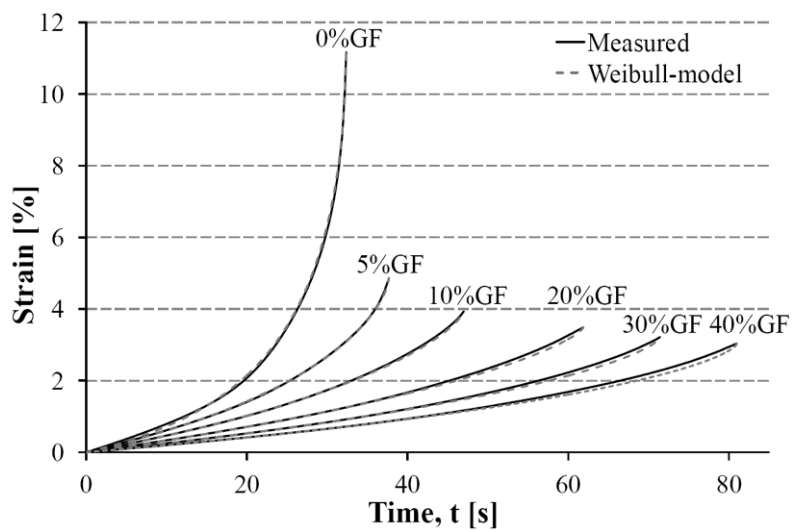


Figure 6. Averaged tensile test curves and their Weibull distribution based approximation

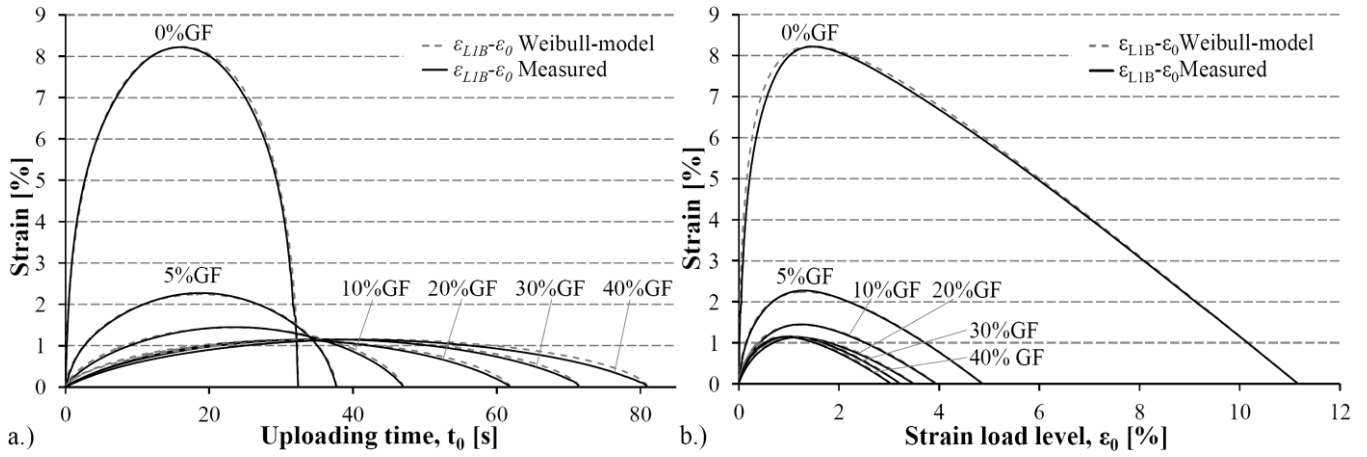


Figure 7. Weibull-based distribution LVE estimation and the measured values of the creep failure strain versus the uploading time (a) and the strain load level (b)

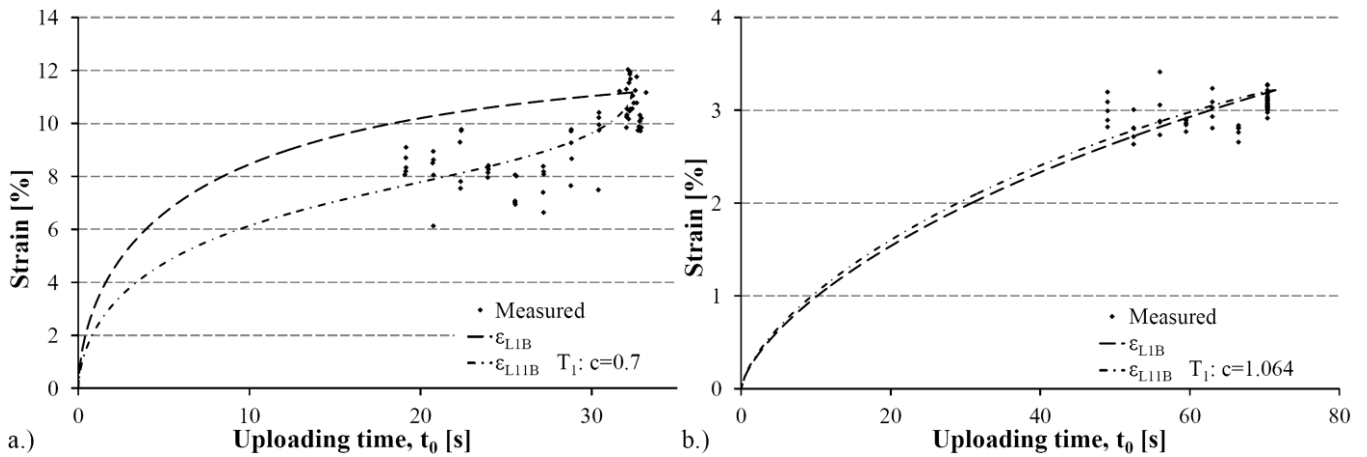


Figure 8. Measured values of the creep failure strain versus the uploading time and their primary and secondary LVE estimations for the neat PP (a) and the 30%GF/PP composite (b)

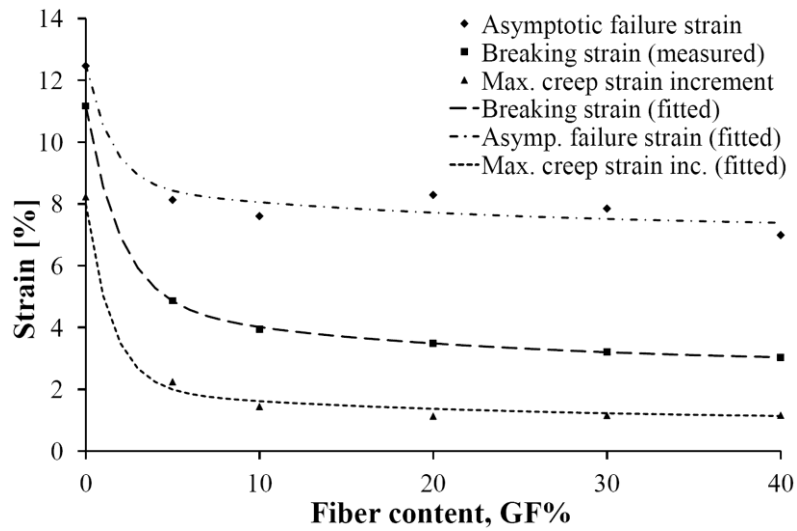


Figure 9. Measured and modelled breaking strain, asymptotic value of the creep failure strain, and maximum value of the creep strain increment versus fibre content

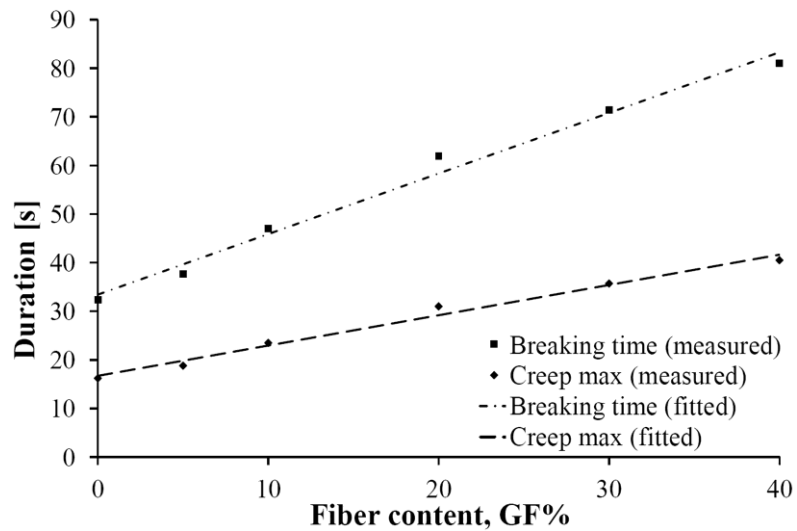


Figure 10. Measured and approximated values of the breaking time and the creep time belonging to the maximum of the creep strain increment versus fibre content

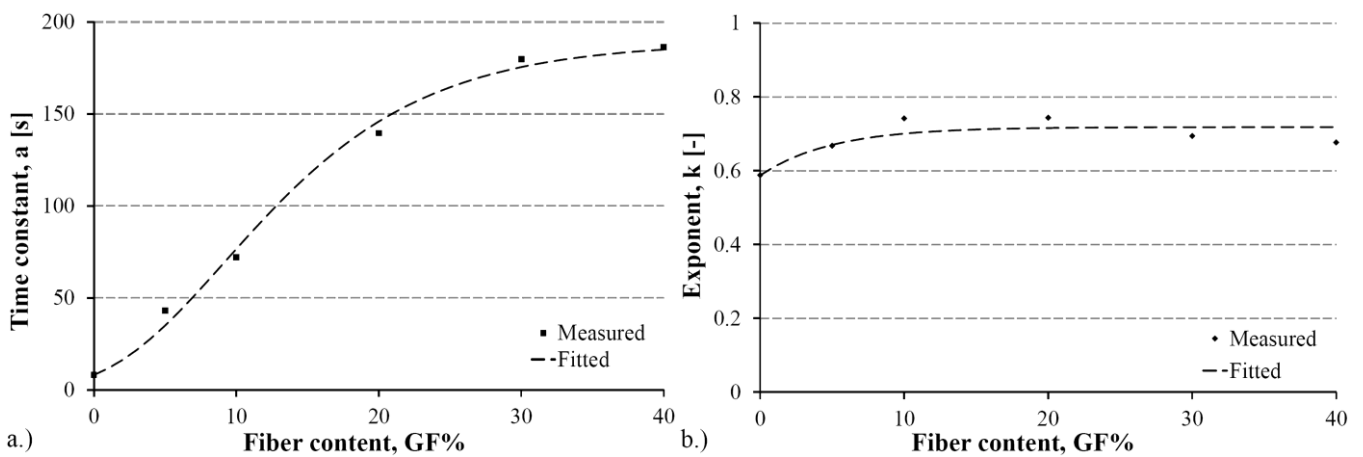


Figure 11. Scale (a) and modulus (b) factors versus fibre content